

ESTIMATION OF TIME DELAYS FROM TWO BLENDED LIGHT CURVES OF GRAVITATIONAL LENSES

A. Hirv, T. Eenmäe, L. J. Liivamägi and J. Pelt
Tartu Observatory, Tõravere, 61602, Estonia

Received 2007 March 28; accepted 2007 June 14

Abstract. Long time photometric monitoring programs of gravitational lens systems are often carried on using modest equipment. The resolution of such observations is limited and some of the images may remain unresolved. It may be still possible to find a full set of time delays from such a blended data. We discuss here a particular but interesting case when we have two light curves that both are blends. A suitable computational algorithm is developed and tested to work with computer-generated model light curves. Our method combines both blended sequences using the hypothetical time delays between the initial components of the light curves as free input parameters. The combined curves are then compared using statistical distance estimation. It occurs that using an assumption of equal magnification ratios between the components of the blends, we can indeed recover the whole set of time delays.

Key words: cosmology: observations – gravitational lensing – methods: statistical

1. INTRODUCTION

To find the time delays caused by differences in light paths of a gravitational lens system, we need at least some recognizable features in the observed light curves. As the longest delays in some systems can be hundreds of days, we need to have sufficiently long measurement sets. Long-time monitorings of such systems are feasible with telescopes of modest size and resolution. The best example of this kind of photometry is the long time series obtained by Schild et al. (1997). The constrained resolution can be also a problem for some large scale photometry programs. This motivates us to investigate possibility to recover time delays from the data which are not fully resolved. The general scheme of the relevant algorithms was developed in Hirv et al. (2007).

In the following we will focus on the case of four original images whose unresolved observations result in two blended light curves. To recover the full set of time delays, we will use the principles of computing the dispersion spectra introduced in Pelt et al. (1994) and Pelt et al. (1996). Hirv et al. (2007) developed a similar method and applied it to a three-image system where two original light curves were blended together but the third curve was fully resolved.

The method of dispersion spectra was singled out as a base for our algorithms because of its conceptual simplicity. There are many other methods available. For the latest see Burud et al. (2001), Koptelova et al. (2006), Vakulik et al. (2006), Cuevas-Tello et al. (2006) and references therein. Some of these new methods can

be generalized to handle blended data. Some critical remarks about the method of dispersion spectra can be found in Gil-Merino et al. (2002) and response to the critique in Pelt et al. (2002).

There are two simplifying implicit assumptions in our treatment below. First, we suppose that the data sets contain a substantial number of observations with sufficient time coverage, and secondly, we totally ignore possibility of distortions due to the effect of microlensing. Consequently, when applying the new method to real observational data, certain care must be exercised.

Our paper is organized as follows. First we introduce the basic ingredients of the new algorithm. Then we present test data generation methods. In the next part we describe the results of the numerical tests and discuss various implementation details which can be of use for the prospective users of the new method. The relevant software modules may be obtained from the authors.

2. THE METHOD

2.1. The continuous case

Let us have a quasar image split into four components by an intervening gravitational lens. Formally we have four functions of the quasar source variability $q(t)$: $f_k(t) = a_k q(t - t_k)$, $k = 1, \dots, 4$, where a_k are the magnification coefficients and t_k are the *flight times* due to different flight paths. Our observational equipment can supposedly record only two images as the close pairs of f_1, f_2 and of f_3, f_4 are blended together due to insufficient resolution. Thus the corresponding signals $g_1(t)$ and $g_2(t)$, that we are going to observe, are the following functions of the source variability $q(t)$:

$$g_1(t) = a_1 q(t - t_1) + a_2 q(t - t_2), \quad (1)$$

$$g_2(t) = a_3 q(t - t_3) + a_4 q(t - t_4). \quad (2)$$

As the spatial separation of f_1 and f_2 is small, we may assume, that $a_1 \approx a_2$ and similarly $a_3 \approx a_4$ for f_3 and f_4 . The amplification ratio between $g_1(t)$ and $g_2(t)$ is then $a \approx a_1/a_3$. Let the time delay between $f_1(t)$ and $f_2(t)$ be $\Delta a = t_2 - t_1$, and the time delay between the components of the second image $\Delta b = t_4 - t_3$. These delays are typically rather short due to nearby flight paths for the component images. As the paths of $f_1(t)$ and $f_3(t)$ differ significantly (larger spatial separation), the corresponding delay $\Delta c = t_3 - t_1$ is the longest one. Now we can rewrite the Eqs. (1) and (2) in terms of the first subimage $f_1(t)$ and relative time delays:

$$g_1(t) = f_1(t) + f_1(t - \Delta a), \quad (3)$$

$$g_2(t) = f_1(t - \Delta c) + f_1(t - \Delta c - \Delta b). \quad (4)$$

To keep things easier to follow we did not multiply the Eq. (4) by the amplification ratio a . The fact, that g_1 and g_2 may have different baselines and amplitudes is taken into account in our computational (matching) algorithm. As a schematic example of the initial variability, the $f_1(t)$ is shown as a single-peaked function in Figure 1. Shifting it by delays Δa , Δb and Δc and adding the results as in the Eqs. (3) and (4) we get the double peaked blends $g_1(t)$ and $g_2(t)$ of the source variability.

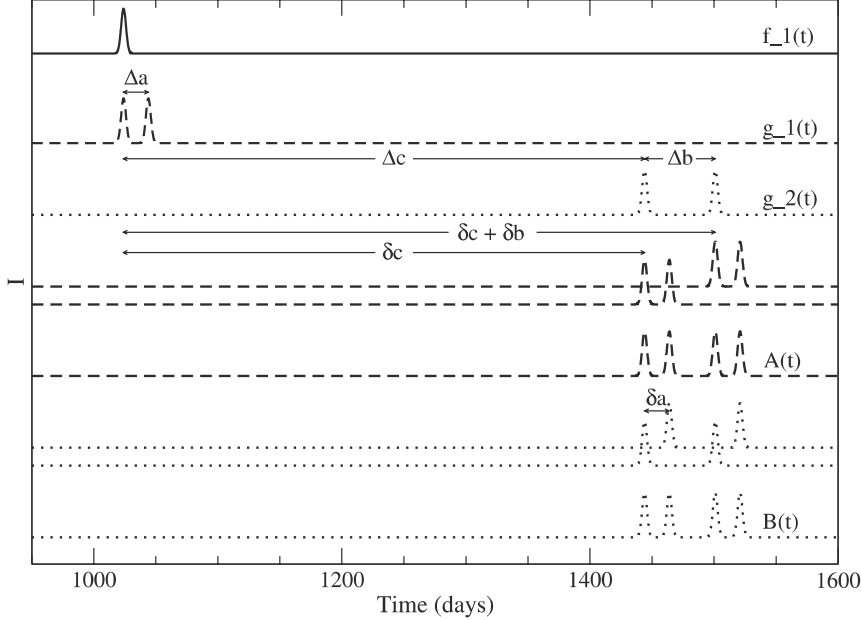


Fig. 1. Graphical explanation of the method. See text for details.

To recover all the three independent time delays Δc , Δa and Δb hidden in the light curves $g_1(t)$ and $g_2(t)$, we will combine the data using three trial delays δc , δa and δb into artificial blends $A(t)$ and $B(t)$:

$$A(t) = g_1(t - \delta c) + g_2(t - \delta c - \delta b), \quad (5)$$

$$B(t) = g_2(t) + g_1(t - \delta a). \quad (6)$$

If it happens, that $\delta c = \Delta c$, $\delta a = \Delta a$ and $\delta b = \Delta b$, the difference of $A(t)$ and $B(t)$ vanishes to zero and this is the situation we are going to search for. The composition of the artificial blends $A(t)$ and $B(t)$, when the trial delays match the initial delays, is also shown in Figure 1. For clarity we plotted the components of the artificial blends before and after adding. Blends and components that have the same origin are plotted using the same line type. As we can see, artificial blends have the same profile, when trial delays correspond to the initial ones, and the difference between $A(t)$ and $B(t)$ vanishes. This is the idea of our method in terms of the continuous and noise-free light curves. Next we will see, how this kind of construction can be used for real noisy and sampled data. (For detailed discussion on adding and subtracting of sampled noisy time-series see Hirv et al. 2007).

2.2. The sampled case

To build the combined sums from input data sequences (time, magnitude, statistical weights) $t_n, g_n, W_n, n = 1, 2, \dots, N$ and the time shifted versions of them

$t_m, g_m, W_m, m = 1, 2, \dots, M$, we form a table of triples

$$\frac{t_n + t_m}{2}, g_n + g_m, W_{n,m}, \quad (7)$$

using data from the sequence g_1 for blend A and data from the sequence g_2 for blend B . Values $W_{n,m}$ are computed as combined weights:

$$W_{n,m} = S_{n,m} \frac{W_n W_m}{W_n + W_m}, \quad (8)$$

where $S_{n,m}$ is the *downweighting function*:

$$S_{n,m} = \begin{cases} 1 - \frac{|t_n - t_m|}{\sigma}, & \text{if } |t_n - t_m| < \sigma, \\ 0, & \text{if } |t_n - t_m| > \sigma, \end{cases} \quad (9)$$

and σ is the *downweighting parameter*, which depends on sampling (it can be prefixed or chosen using trial calculations).

Next, by varying trial delays δc , δa and δb the artificial blends A and B are recalculated and weighted sums of squared differences between them are found:

$$D^2 = \min_{\alpha, \beta} \frac{\sum_{n,m} (\alpha A_n + \beta - B_m)^2 W_{n,m}^{A,B}}{\sum_{n,m} W_{n,m}^{A,B}}. \quad (10)$$

We may call D^2 as the *statistical distance* between A and B . Regression coefficients α and β are needed, because artificial blends may have different baselines and magnification. They are recalculated for every set of trial delays. The combined weights for D^2 :

$$W_{n,m}^{A,B} = S_{n,m} \frac{W_n^A W_m^B}{W_n^A + \alpha^2 W_m^B}, \quad (11)$$

are formed from W_n^A and W_m^B which are calculated using Eq. 8 for both artificial blends.

By varying trial delays δc , δa and δb over pre-given grids, we are searching for the global minimum of statistical distance D^2 which corresponds to the recovered time-delay system. The weights contain parameter α to be estimated, consequently we need an iterative scheme to get final dispersions. First we set $\alpha = 1$ in Eq. (11), then solve linear weighted least squares equations to get estimates for α and β . After that we insert a new value of α into weights and recompute. Normally this process converges in 3–4 steps. A similar approach was used by Hirv et al. (2007).

2.3. Features and difficulties of the method

There are three additional issues, which we have to bear in mind, before starting actual calculations.

- Recovering the time-delay system is a degenerate problem. The mirrored values of short delays Δa and Δb are also valid. For a single data set we can get four equally correct solutions: Δc , Δa and Δb ; $\Delta c + \Delta b$, Δa and $-\Delta b$; $\Delta c - \Delta a$, $-\Delta a$ and Δb ; and $\Delta c - \Delta a + \Delta b$, $-\Delta a$ and $-\Delta b$. (Interchanging g_1 and g_2 gives us four additional sets of solutions, where Δc is mirrored and Δa and Δb are interchanged.) All the four solutions form detectable minima in the three-dimensional

grid of D^2 values. For finite sequences these minima may have slightly different merit function values. Our method just finds formally the deepest minimum and corresponding time-delay system. The recovered set of time delays may be considered real, if it shows up as a visually noticeable minimum in the two-dimensional slice of statistical distance values (see low-noise part of Figure 3). Formal significance estimation is possible using the bootstrap-type techniques and ideas from Pelt et al. (1996).

- Our method does not work if $|\Delta a| = |\Delta b|$. Both blends are then similar, and we can recover only the largest delay Δc using simplest “one-dimensional” dispersion spectra. Having a value for the long delay it is then in principle possible to recover the short delay (the same for both blends) from the combined data using the methods described in Geiger & Schneider (1996). The combining of two photometric series with estimated long delay allows sometimes (if microlensing effect is negligible) to get a data set with twice the original sampling rate.

The case of $|\Delta a| = |\Delta b|$ may be promptly recognized from the plot of D^2 values – one of the four possible solutions has a characteristic distribution along straight line of D^2 values (see for instance Figure 5). We may also hit an arbitrary solution corresponding to mirrored arbitrary short delays, which shows up as a normal minimum in the two-dimensional plot of D^2 values. Hence the solutions where $|\delta a| \approx |\delta b|$ should be handled with care. A three-dimensional plot of D^2 values would be useful here.

The tests with simulated data-sets showed, that for a reasonably good sampling and low noise even one day differences between Δa and Δb values can be resolved.

- The process of calculating the D^2 values in the algorithm for two blends is different from its analog for a clean curve and a blend. The calculation of D^2 involves differences of the observed data sums. In the case of a clean image and a blend, we have differences of original data points and combined sums. From what follows that total scatter of the differences in the new method is somewhat higher and statistical stability is lower. Consequently, the two blend method demands data with higher quality.

Our method for two blends recovers the time delays correctly also for a clean image and a blend. Because of different sensitivity to noise, it is sensible to use proper method for the nature of a given problem. For unknown nature, it is worth trying both algorithms for the given input data.

2.4. Data analysis

The procedure of analyzing real data includes the following steps. At first, we need to find a suitable downweighting parameter σ for a given data sampling. Next, we should verify if the noise level of our data is under the noise value our method can handle. And finally, we may analyze the observed curves to recover the time-delay system.

We can use an interactive simulation for estimating the suitable downweighting parameter for real observational data. First, we generate artificial noise-free curves with some pre-given time delays, using the sampling of our real data. Then starting from small downweighting parameter (say $\sigma = 0.5$), we move on towards larger ones and recalculate the plot of D^2 and recover the time delays for each σ . In general, there is an optimal σ for a given sampling which recovers the time delays correctly and produces clearest minimum on the D^2 surface. Once we have found the optimum, further enlargement of downweighting parameter will not improve

the results. It is also possible, that for a given sampling and time-delay system, there is no working downweighting parameter at all. Even for a correctly estimated value of σ the overall success of the algorithm depends on the length of the time series, noise level and absolute values of actual time delays. For the best results, σ should not be larger than half of the shortest time delay we are going to recover. See also Hirv et al. (2007) where the estimation of the correct σ is presented in some detail.

To verify if the noise level of our data is tolerably low for the method, we may use the same simulated curves that were used for estimating the σ parameter. Taking these model sequences, adding gradually increasing levels of Gaussian noise and recovering the foreknown time delays, we can find the maximum tolerable noise level for our algorithm. Then we compare the signal to noise ratio (S/N) of the observational data and test data which had the maximum tolerable amount of noise. The S/N of observational data should be higher than for the test data.

Once we have found that further analysis of the observational data is reasonable, we perform the three-dimensional search for the minimum of D^2 . The values of our trial parameters δa , δb and δc which correspond to the minimum of D^2 , can be considered as the real recovered time-delay system, if all the presented above issues and complications were taken into account.

3. GENERATING TEST DATA

The quasar source variability q_n, t_n is simulated using simple random walk. A randomly chosen value of ± 1.0 is assigned cumulatively to each step in the intensity scale. The initial time points are generated by using random step sizes from the interval $[0.2, 1.8]$ days. Then the quasar signal is shifted in time by delays Δa , Δb and Δc and blended as in the Eqs. (3) and (4). For blending the intensities, linear interpolation is used. The blend g_2 is multiplied by amplification ratio $a = 0.8$ to make things more realistic (the inherently important assumption of the method is that both components of a given blend have nearly equal magnification coefficients). Both blends, g_1 and g_2 , can be resampled using generated or real observed sequences of time points and linear interpolation. Finally, the Gaussian noise is added to the model observational noise. One example of the generated curves is shown in Figure 2.

4. TESTING THE METHOD

4.1. Simulated data

Currently we do not have observational sequences at our disposal, that are long enough, sampled well and have noise level our method can work with. So, to test the method, we had to build artificial sequences. We generated a 4300 day long (2740 points) noise-free dataset with random sampling which had only daylight caps; $\Delta c = 420.2$, $\Delta a = 20.2$, $\Delta b = 56.5$ days and $a = 0.8$. This set was also used for estimating the optimal downweighting parameter for the given sampling. Different levels of Gaussian noise were added to the computed curve to check our method's stability against noise. This set with added Gaussian noise is shown in Figure 2.

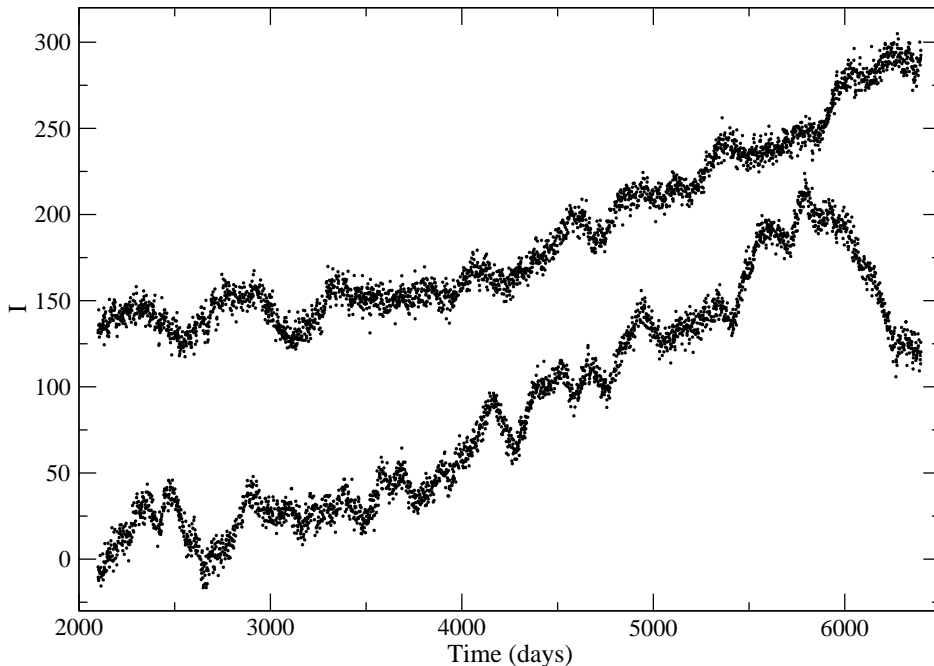


Fig. 2. The computer-generated blends g_1 (lower curve) and g_2 (shifted up by 130 units). $\Delta c = 420.2$, $\Delta a = 20.2$, $\Delta b = 56.5$ days and $a = 0.8$. The standard deviation of the added Gaussian noise is 5 units.

For our test data the optimal downweighting parameter was $\sigma = 1.5$. To find the maximally tolerable level of noise, we performed a three-dimensional search for time delays, using the one day step size and the following limits for trial delays: $\delta c = 370 \dots 470$, $\delta a = -30 \dots 70$, $\delta b = 6 \dots 106$. The results of noise tests are given in Table 1 and in Figure 3. As we can see, the Gaussian noise with a standard deviation of two units introduces one day error in the estimates of Δc and Δa ; the Gaussian noise with

Table 1. Recovered time delays depending on the added Gaussian noise.

Noise (stdev)	Δc	Δa	Δb
0.0	400	-20	57
1.0	400	-20	57
2.0	401	-19	56
3.0	401	-18	56
4.0	401	-18	57
5.0	417	19	59
6.0	426	27	52
7.0	426	19	48
8.0	421	26	58
9.0	413	20	50
11.0	414	42	84
14.0	442	43	31

a standard deviation of six units gives us a seven day error in the estimate of Δa ; and a noise level of 11 units makes an error in the estimate of Δa comparable to its original value. The signal to noise ratio was $S/N = 30$ in the case of standard deviation of six units. Hence, for a reasonably well sampled real data we should keep the $S/N \geq 30$ for the method to work properly.

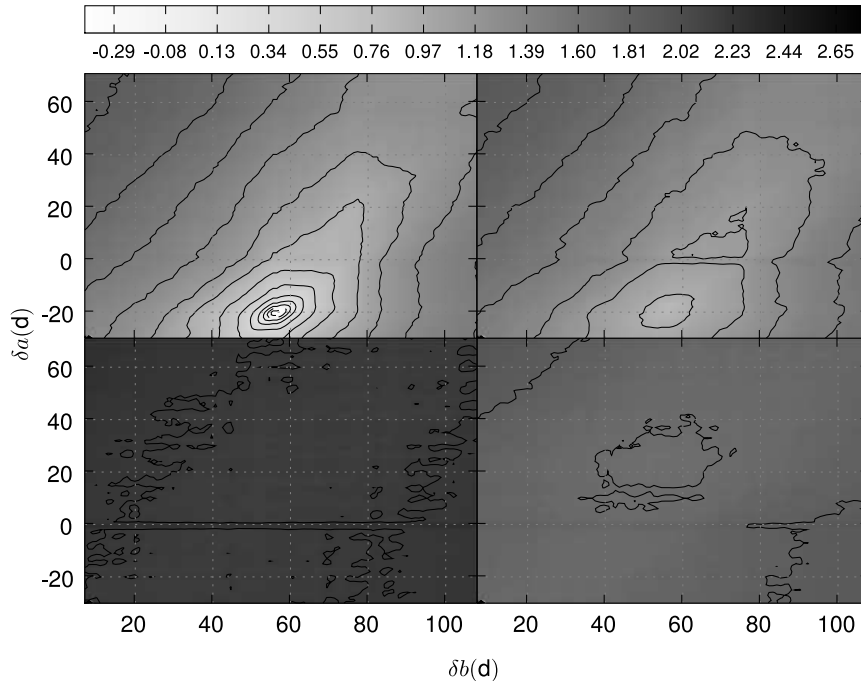


Fig. 3. Vanishing of the detectable minimum on the D^2 surface due to observational errors. The standard deviations of the added Gaussian noise are (clockwise from upper left): 0.0, 2.0, 6.0 and 11.0. Values on the color key represent the $\log(D^2)$ and spacing of the contours. The same type of color key is used in all two-dimensional plots.

4.2. Problem with Schild's data

In Hirv et al. (2007) we applied the algorithm for a clean image and a blend to the observational data by Schild et al. (1997). As we got then interesting results, we considered applying the algorithm for two blends as well. The optimal downweighting parameter $\sigma = 1.5$ for Schild's time series was found. Next we found also the noise tolerance of the method for two blends using Schild's sampling. Having real but bad sampling, where the points to days ratio is 0.2 and large gaps are included, the working noise tolerance decreased to 3.0 units (standard deviation). The corresponding signal to noise ratio was $S/N = 50$. Next we compared the signal to noise ratio of the Schild's data and of our simulated curves. Unfortunately the S/N ratio for Schild's data occurred to be lower than the ratio for good enough simulated curves. Because of that we cannot use assumption about two blends for finding time delays from Schild's data. Schild's noise level was tolerable for the algorithm for a blend and a clean image, but not for the algorithm for two blends. (For the explanation see Section 2.3.)

4.3. The $|\Delta a| \approx |\Delta b|$ case

Having well sampled data and low noise, it is still possible to get a solution for very close short delays. For example, we took $\Delta c = 420.2$, $\Delta a = 56.5$, $\Delta b = 50.1$ days having a good sampling with daylight caps only and no noise. The given time delays were recovered correctly. The resulting plot of D^2 values is shown in

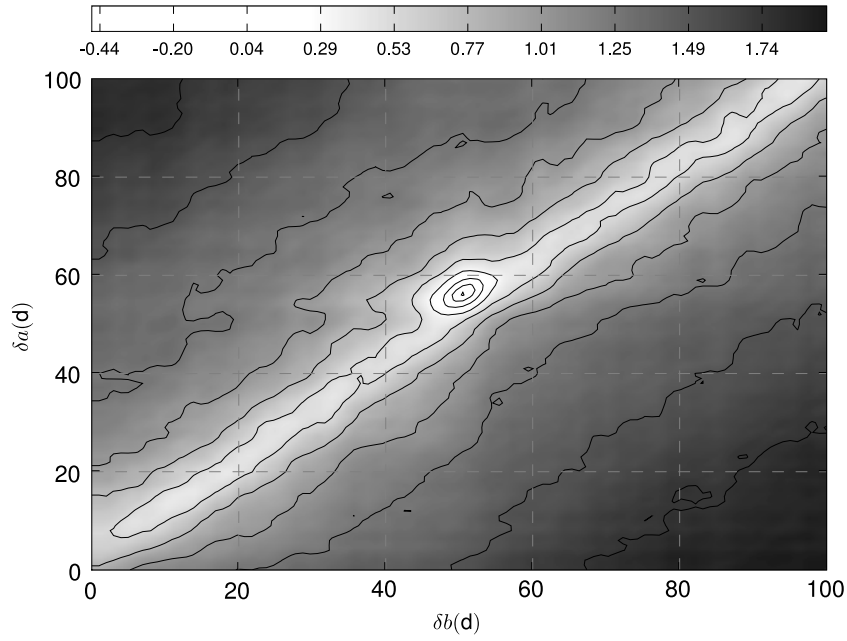


Fig. 4. D^2 values for very close short delays. $\Delta c = 420.2$, $\Delta a = 56.5$, $\Delta b = 50.1$ days and $a = 0.8$.

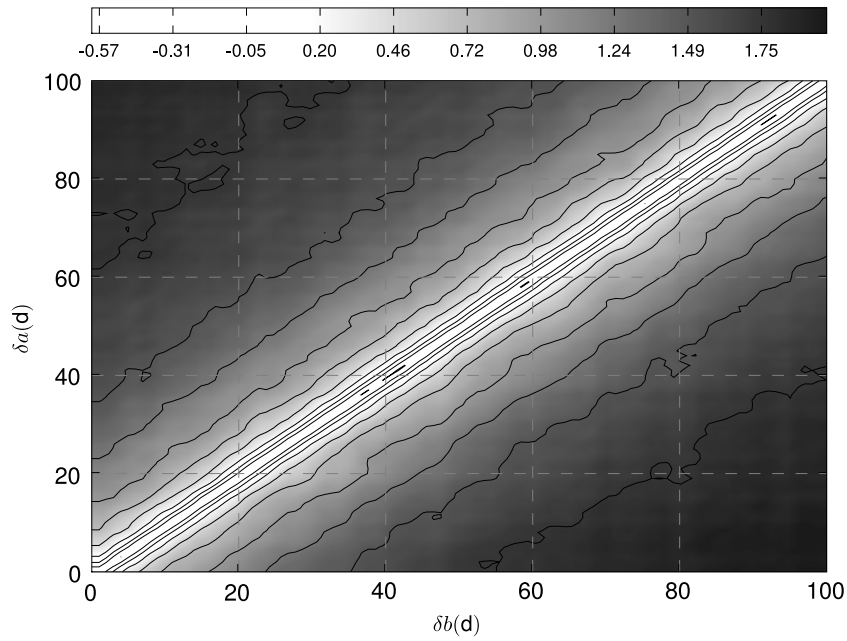


Fig. 5. D^2 values for $\Delta a = \Delta b = 20.2$, $\Delta c = 420.2$ days and $a = 0.8$.

Figure 4. Even a one day difference between Δa and Δb is still tolerable for the method, but then the minimum on the D^2 surface is not very convincing indeed.

The singular situation, where initial $\Delta c = 420.2$, $\Delta a = 20.2$, $\Delta b = 20.2$ days is shown in Figure 5. We can see a characteristic distribution along straight line of D^2 values and no minima, but this is not always the case, as was discussed in Section 2.3.

5. CONCLUSION

A method for estimating time delays from two blended light curves was developed and tested. As the new algorithm is more sensitive to observational errors than is the algorithm for a clean image and a blend, we were not able to confirm the interesting results for real Schild's data obtained in Hirv et al. (2007).

Although we did not have observational data good enough for analysis, all the steps of recovering time delays from real data were simulated as realistically as possible. For planning the real observations, one should repeat similar simulations to establish realistic limits for observational errors and sampling.

We believe that two new algorithms and the classical method of dispersion spectra form a useful toolset to analyze data which will flow out from the extensive photometric programs planned. If enough data and sufficient computing power will be available then we can set up a new kind of searching program. First, we select from a general database the records, where two nearby measured images are variable, then we apply the delay estimation schemes. If we find that two curves can be described as time shifted replicas of the single source curve or blends with proper delay structure then the follow up spectroscopy can be called upon.

ACKNOWLEDGMENTS. This work was supported by the Estonian Science Foundation grants Nos. 6810 and 6813. Special thanks are to Krista Alikas for valuable comments.

REFERENCES

- Burud I., Magain P., Sohy S., Hjorth J. 2001, *A&A*, 380, 805
 Geiger B., Schneider P. 1996, *MNRAS*, 282, 530
 Gil-Merino R., Wisotzki L., Wambsganss J. 2002, *A&A*, 381, 428
 Hirv A., Eenmäe T., Liimets T., Liivamägi L. J., Pelt J. 2007, *A&A*, 464, 471
 Koptelova E. A., Oknyanskij V. L., Shimanovskaya E. V. 2006, *A&A*, 452, 37
 Pelt J., Hoff W., Kayser R., Refsdal S., Schramm T. 1994, *A&A*, 286, 775
 Pelt J., Kayser R., Refsdal S., Schramm T. 1996, *A&A*, 305, 97
 Pelt J., Refsdal S., Stabell R. 2002, *A&A*, 389, L57
 Cuevas-Tello J. C., Tiño P., Raychaudhury S. 2006, *A&A*, 454, 695
 Schild R., Thomson D. J. 1997, *AJ*, 113, 130
 Vakulik V., Schild R., Dudinov V. et al. 2006, *A&A*, 447, 905